Journal of Power Sources 194 (2009) 1036–1042

Contents lists available at ScienceDirect

Journal of Power Sources

journal homepage: www.elsevier.com/locate/jpowsour

Surface modified $LiFePO_4$/C nanocrystals synthesis by organic molecules assisted supercritical water process

Dinesh Rangappa[a,*], Masaki Ichihara[b], Tetsuichi Kudo[a], Itaru Honma[a,*]

[a] Energy Technology Research Institute, National Institute of Advanced Industrial Science and Technology (AIST), Umezono 1-1-1, Tsukuba, Ibaraki 305-8568, Japan
[b] Material Design and Characterization Laboratory Institute for Solid State Physics University of Tokyo, 5-1-5 Kashiwanoha, Kashiwa, Chiba 277-8581, Japan

ARTICLE INFO

Article history:
Received 3 April 2009
Received in revised form 8 June 2009
Accepted 15 June 2009
Available online 24 June 2009

Keywords:
$LiFePO_4$
Nanoelectrode
Surface modification
Supercritical water
Size control

ABSTRACT

A novel one-pot synthesis strategy has been developed to prepare organic modified $LiFePO_4$/C nanocrystals under organic molecules assisted supercritical water (SCW) conditions. Powder X-ray diffraction (XRD) and high-resolution transmission electron microscopy (HR-TEM) results indicate that crystalline $LiFePO_4$ nanocrystals are formed under SCW conditions. The smallest ever reported $LiFePO_4$ nanocrystals with size ca. 15 nm are obtained by one-pot synthesis at 400 °C in short reaction time. The SCW conditions along with suitable surfactants facilitated the in situ organic modification of $LiFePO_4$ with controlled particles size. Further, addition of CNT during the SCW synthesis helps in developing conductive carbon coating on the surface after heat treatment.

1. Introduction

Among the lithium ion secondary battery electrode materials, the olivine-structured lithium iron phosphate ($LiFePO_4$) has attracted extensive attention due to its low cost, low toxicity, good thermal stability and high charge/discharge capabilities [1]. In spite of these advantages, it is difficult to exploit its full capacity for commercial applications, because of its poor electronic conductivity and slow Li^+ ion diffusion in the olivine structure [2]. Many attempts have been made to overcome these problems by coating the $LiFePO_4$ particles surface with electronically conductive phase (carbon, polymer or metal, etc. [3,4]), doping with hetero-atoms [5] or reducing the particles size [6]. Recently, several synthetic routes have been reported for the preparation of $LiFePO_4$/C nanoparticles, for instance mechanical alloying [7,8], sol–gel method [9,10], co-precipitation [11], microwave process [12], hydrothermal route [12,13,1], emulsion drying synthesis [14,15], carbo-thermal reduction method [16], vapor deposition [17], spray solution technology [18], and so on. All these methods have produced $LiFePO_4$ nanoparticles in the size range of 40–200 nm. However, it has been still a challenge to prepare the $LiFePO_4$ nanocrystals with size less than 20 nm due to the lack of suitable synthetic technique that facilitates the size control of the $LiFePO_4$ particles. For this purpose, an in situ surface modification of nanoparticle with surfactants is one of the best solutions, which has been rarely considered for this material.

Recently, Adschiri et al. have developed a versatile pathway towards size and shape controlled metal oxide nanocrystals exploiting the properties of supercritical water (SCW) [19,20]. Using the organic ligand molecules that are miscible with the SCW, the nanocrystals surface would be capped with ligand molecules, inhibiting the crystal growth and agglomeration leading to the formation of small and well-dispersed nanoparticles [21].

In this study, we are reporting a novel one-pot synthesis strategy for the synthesis and in situ surface modification of $LiFePO_4$/C nanocrystals by organic molecules assisted supercritical water method. The smallest ever reported $LiFePO_4$ nanocrystals (<15 nm) have been synthesized at 400 °C in a short reaction time of about 10–15 min.

2. Experimental

2.1. Preparation of $LiFePO_4$/C nanocrystals

The $LiFePO_4$/C nanocrystals were synthesized using $FeC_2O_4 \cdot 2H_2O$, $NH_4H_2PO_4$, LiOH, and ascorbic acid (all from Aldrich). The starting precursor solution was prepared in 1:1:1 molar ratio using source materials. First, $NH_4H_2PO_4$ and $FeC_2O_4 \cdot 2H_2O$ (0.1 mol l^{-1}) were dissolved separately in water. A solution of LiOH (0.1 mol l^{-1}) and desired amount of ascorbic acid were added to this mixture. Later a desired amount of oleic acid in ethanol solution was mixed with the starting precursor solution and stirred well in a beaker for

* Corresponding authors. Tel.: +81 298615648; fax: +81 298615799.
E-mail addresses: dinesh.r@aist.go.jp (D. Rangappa), i.homma@aist.go.jp (I. Honma).

0378-7753/$ – see front matter © 2009 Elsevier B.V. All rights reserved.
doi:10.1016/j.jpowsour.2009.06.042

1 h. The amount of ethanol used in this solution was about 10 volume percent. The surfactant to precursor molar ratio was 1:10–20. In a typical synthesis, 5 ml of precursor solution was charged in 10 cm^3 volume stainless steel reactor and heated up to 400 °C temperature and 40 MPa pressure. After 10–30 min reaction, the reactor was quenched with cold water to stop the reaction. A pale green to grayish color product was collected by washing the reactor with ethanol followed by repeated centrifugation with ethanol to remove the unwanted salts. The organic modified and/or carbon coated particles were extracted by washing samples with hexane. Resultant products were dried in a vacuum dry oven at 120 °C for 6 h in order to eliminate residual water from the particle. Later, this product was heat treated at 500 °C for 2 h in an Ar and H_2 gas atmosphere to convert organic molecules/carbon on $LiFePO_4$ surface to carbon.

2.2. Analytical characterization

The crystal structure was examined by X-ray diffraction (XRD) analysis with a Bruker AXS D8 Advance instrument using Cu Kα radiation. The morphology of the film was examined by field emission scanning electron microscopy (FESEM; Carl Zeiss Gemini Supra) and by high-resolution transmission electron microscopy (HR-TEM; JEOL JEM-2010F). Infrared (IR) spectra of the composite materials were recorded by using an FT/IR-6200 IR spectrophotometer (JASCO Corp., Tokyo, Japan). Raman spectra were recorded in the backward geometry on a NIHON BUNKO Ventuno spectrometer (NSR-1000DT) at room temperature. The powder samples were excited by using the 632.8 nm wavelength line from a He–Ne laser.

2.3. Electrochemical characterization

We studied the electrochemical properties of $LiFePO_4$ nanoparticles by assembling a beaker type three electrode cell. The samples were dried overnight at 105 °C in vacuum before assembling the cell. The dried $LiFePO_4$ sample was mixed and ground with acetylene black, CNT and Teflon (poly(tetrafluoroethylene)) binder in the weight ratio of 75:10:10:5. The prepared paste was spread uniformly on a 0.1 cm^2 stainless steel SUS sheet (100 mesh) using the doctor-blade method. The cathode loading was 4–5 mg cm^{-2}. Li metal on stainless steel SUS mesh was used as a counter and reference electrodes. The electrolyte consisted of solution of 1 M $LiClO_4$ in ethylene carbonate (EC)/diethyl carbonate (DEC) (1/1 by volume). The cell assembly was carried out in a glove box filled with high purity argon gas. The charge–discharge tests were performed with a Solartron Instrument Model 1287 controlled by a computer in a potential range of 2.0–4.5 V versus Li under different current densities.

3. Results and discussion

3.1. Crystallographic analysis

The powder XRD patterns of the $LiFePO_4$ nanocrystals are shown in Fig. 1. XRD patterns clearly show single phase formation of an olivine structure $LiFePO_4$ under SCW conditions. All the peaks in the XRD pattern were indexed to an orthorhombic, *Pnmb* space group (JCPDS 40-1499). The $LiFePO_4$ nanocrystals had a good crystallinity directly after the preparation at 400 °C temperature. Generally, a high reaction temperature (>700 °C) or post-heat treatment is necessary to prepare the pure and crystalline $LiFePO_4$ particles [7,9]. It is well known that the $LiFePO_4$ particles prepared in the solution process without heat treatment possess amorphous $LiFePO_4$ or impurities such as Li_3PO_4 or $Fe_2(PO_4)OH$ or α-Fe_2O_3 along with

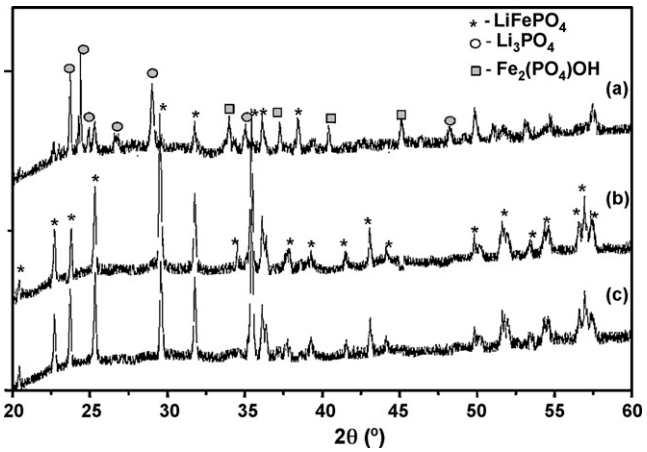

Fig. 1. RD patterns of $LiFePO_4$ nanocrystals obtained at different reaction temperatures: (a) 300 °C, (b) 400 °C and (c) 500 °C.

the $LiFePO_4$ [22]. In the present study, crystalline $LiFePO_4$ nanocrystals were obtained at 400 °C temperature in 10 min reaction time without any post-heat treatment. The effect of reaction temperature (300, 400, and 500 °C) on the crystal phase and crystallinity of the prepared samples are shown in Fig. 1. As evidenced from these XRD patterns, nanocrystals synthesized at 300 °C included some intermediate phases such as Li_3PO_4 and $Fe_2(PO_4)OH$. However, as the temperature increased above 400 °C, the impure phases disappeared showing only olivine $LiFePO_4$. Therefore, we could obtain single phase $LiFePO_4$ nanocrystals at the lowest temperature of 400 °C, taking the advantage of supercritical water conditions. The reaction temperature and time played an important role in the formation of well crystalline $LiFePO_4$ nanoparticles under SCW conditions. This is because; the temperature above critical point favors the crystallinity of particles when compared to the subcritical temperature. In addition, the growth of the nanocrystals was controlled by controlling the reaction time between 10 and 20 min. This could also assisted by the rapid heating and homogeneous reaction atmosphere during the SCW process.

The $LiFePO_4$ nanocrystals formed in the absence of organic molecules showed a relatively sharp peak with the higher intensity (Fig. 2a). Whereas, the XRD pattern of the organic modified $LiFePO_4$ sample showed a decrease in the intensity of the peaks with a peak broadening (Fig. 2b). This suggests that the size of the nanocrystals decreased in the presence of organic molecules. The

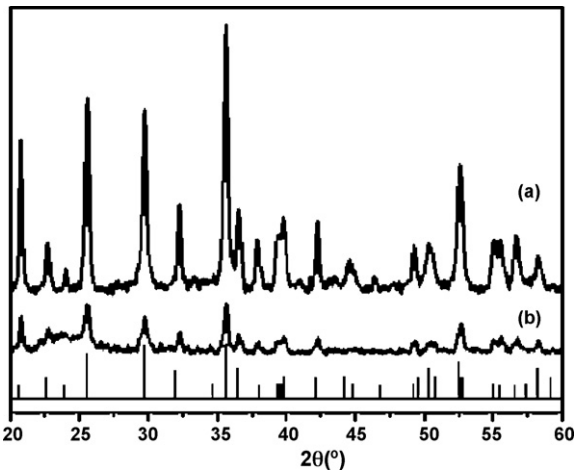

Fig. 2. XRD patterns of $LiFePO_4$ nanocrystals formed: (a) in the absence of organic molecules and (b) in the presence of organic molecules under SCW condition at 400 °C.

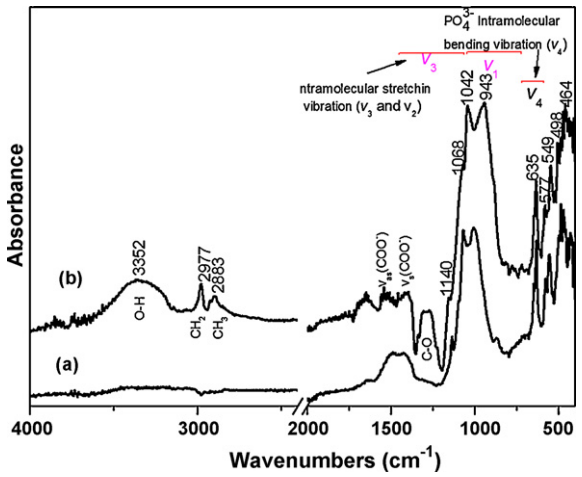

Fig. 3. FTIR absorption spectra of $LiFePO_4$ samples synthesized: (a) in the absence of organic molecules and (b) in the presence of organic molecules under SCW condition at 400 °C.

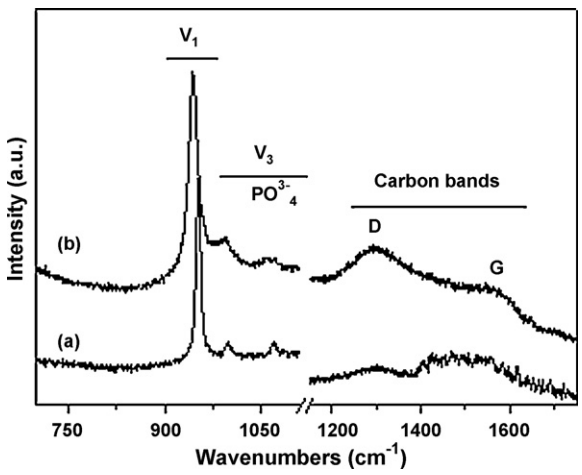

Fig. 4. Raman spectrum of $LiFePO_4$ nanocrystals synthesised: (a) in the absence of organic molecules and (b) in the presence of organic molecules under SCW condition at 400 °C.

crystallite size was evaluated from the 1 3 1 peaks by Scherrer's equation. The average crystallite size of the unmodified $LiFePO_4$ nanocrystals calculated is about 150 nm, while the average crystallite size of nanocrystals synthesized with organic modification is about 18 nm.

3.2. Vibrational spectra of $LiFePO_4$

Formation of $LiFePO_4$ was further confirmed by studying FTIR and Raman vibrational spectra. Spectral assignments for the $LiFePO_4$ vibrations have been previously reported in the literature

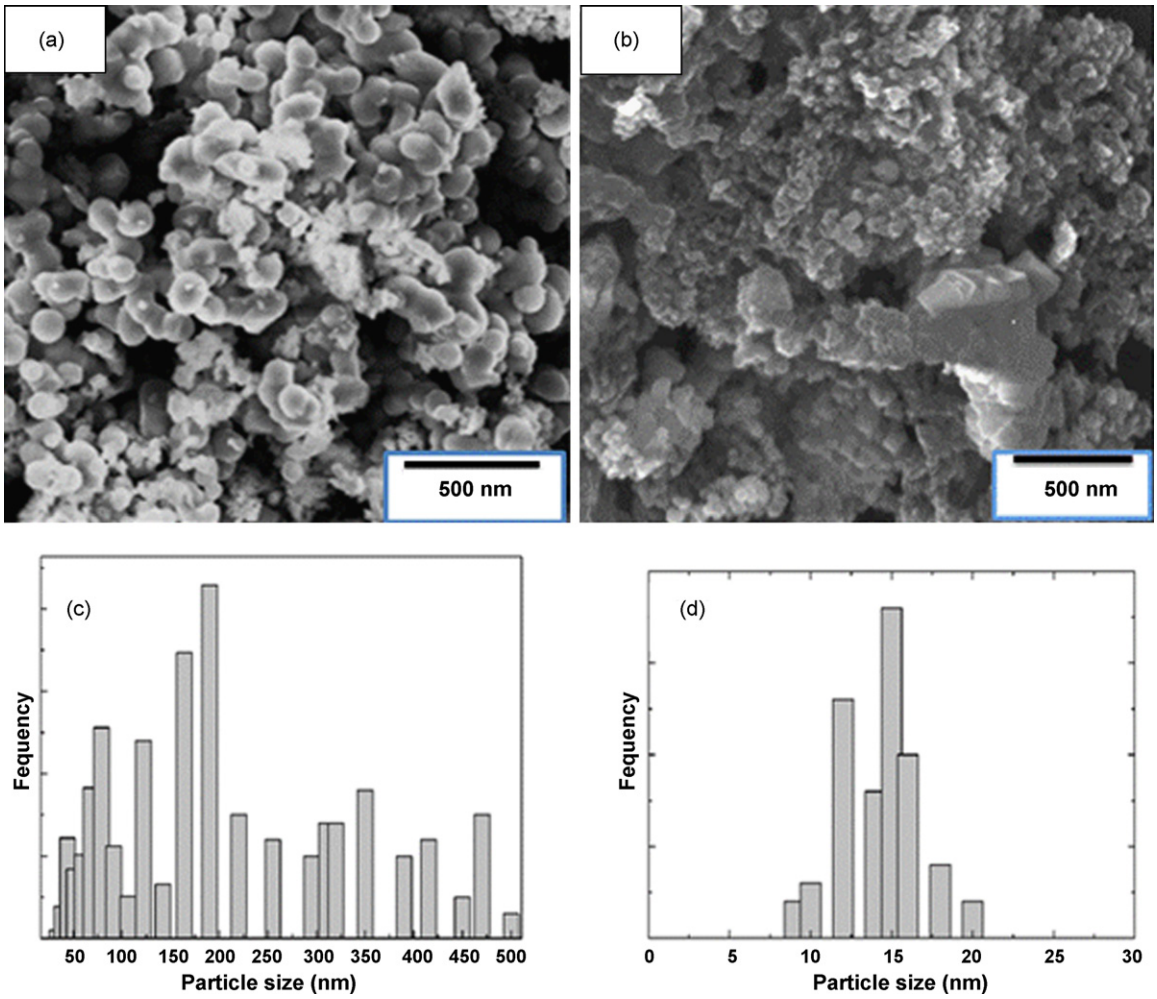

Fig. 5. FESEM images of $LiFePO_4$ nanocrystals synthesized: (a) in the absence of oleic acid molecules and (b) in the presence of oleic acid molecules. The histograms of the particle size distribution, analyzed using the HR-TEM micrographs of $LiFePO_4$ nanocrystals synthesized, (c) in the absence of oleic acid molecules, and (d) in the presence of oleic acid molecules.

and those are compared with currently obtained FTIR and Raman spectra.

3.2.1. FTIR vibrational spectra

The FTIR absorption spectra of as prepared $LiFePO_4$ is shown in Fig. 3. There are two classes of vibrational modes reported for $LiFePO_4$ [23]. Internal mode, originate in the intra-molecular vibrations of PO_4^{3-} anion. The vibration of each PO_4^{3-} anion is correlated to those of the other PO_4^{3-} ions in the unit cell, producing a rich vibrational multiplet structure. The bands observed at 943 and 1042, 1068 and 1140 cm^{-1} are attributed to the intra-molecular stretching (V_1 and V_3) motions of the phosphate anions, respectively. The bands in the region of 643–633 cm^{-1} can be assigned to the bending modes (V_4) of phosphate anions. These bands are strongly coupled and problematic to assign as it involves lithium ion motion. The bands in the region of 500–665 cm^{-1} can be assigned to the lithium ion motion. Fig. 3b shows the FTIR spectra of organic modified $LiFePO_4$ nanocrystals. As we can see in the FTIR spectra, there is no much difference in the vibrational modes (region 500–1150 cm^{-1}) of $LiFePO_4$ when compared to $LiFePO_4$ synthesized in the absence of organic molecules. However, the organic modified $LiFePO_4$ shows the bands in the region 2800–2960 cm^{-1} which are attributed to the C–H stretching mode of methyl and methylene groups (Fig. 3b). The bands at 1532 and 1445 cm^{-1} correspond to the stretching frequency of the carboxylate group, which suggests that the carboxylate group from oleic acid was chemically bonded to the surface of the $LiFePO_4$ nanocrystals. This confirms that $LiFePO_4$ nanoparticles surface was coated with organic ligand during the organic molecules assisted SCW synthesis.

3.2.2. Raman spectra

To further investigate the structure of $LiFePO_4$ and surface coated carbon, Raman spectroscopy analysis was employed. Fig. 4 shows the typical Raman spectrum of $LiFePO_4$ nanocrystals synthesized in the absence and presence of oleic acid in the precursor. The spectrum consisted of a band at 950 cm^{-1} corresponding to the symmetric PO_4^{3-} stretching vibration mode ν_1 in $LiFePO_4$ olivine compound. The bands from 999 to 1071 cm^{-1} are assigned to the stretching vibration mode ν_3 [24]. A broad band at 1350 and 1570 cm^{-1} corresponding to deposited carbon was observed for the $LiFePO_4$ nanocrystals that were synthesized in the presence of oleic acid molecules (Fig. 4b), whereas, these bands were not observed for the $LiFePO_4$ nanocrystals that were synthesized in the absence of oleic acid molecules (Fig. 4a). Doeff et al. pointed out that the bands in this region were composed of four signals, whose locations were 1194, 1347, 1510 and 1585 cm^{-1} [24]. According to their report, the bands at 1347 and 1585 cm^{-1} corresponded to SP^2 graphite like structure. Therefore, Raman spectrum reveals that all bands observed belong to the typical $LiFePO_4$ and semi-graphitic carbon. It should be noted that the semi-graphitic type of carbon was deposited under organic molecules assisted SCW conditions with long reaction time (>30 min). It has been reported that under

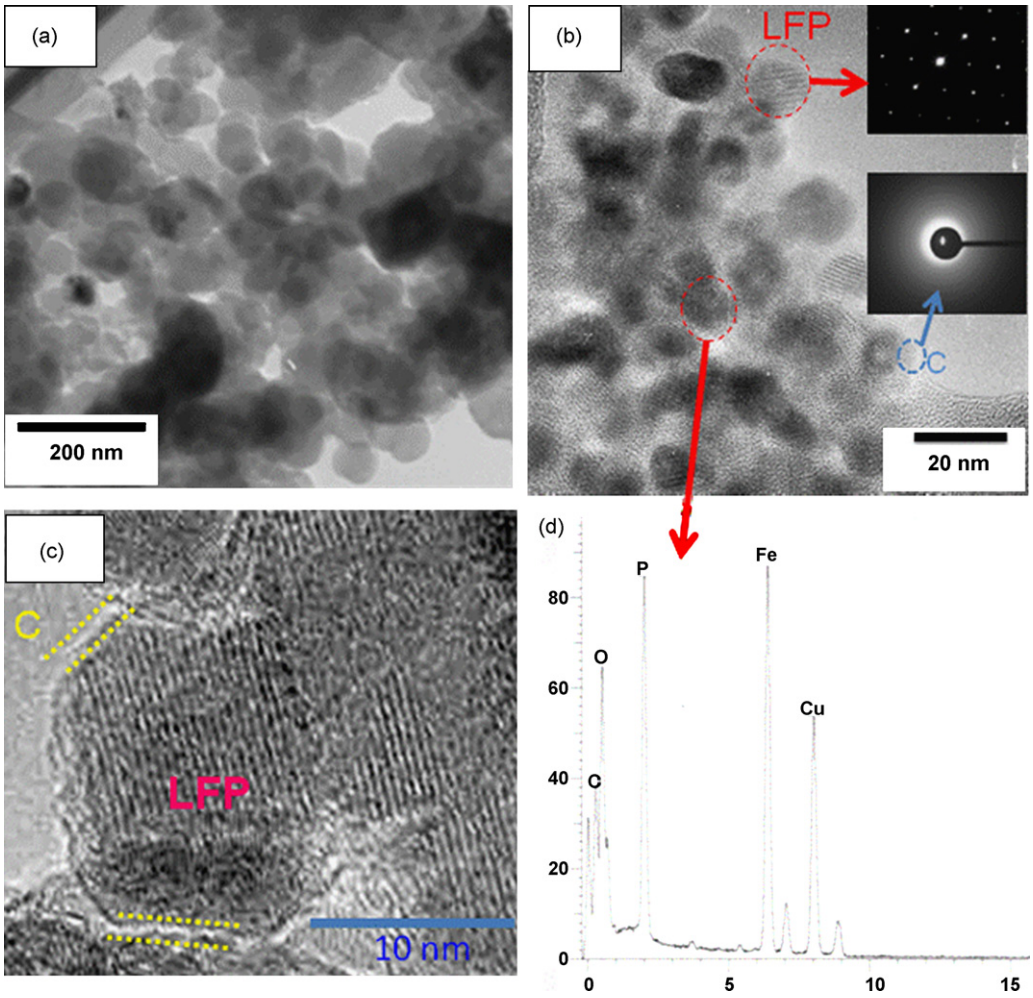

Fig. 6. HR-TEM images of $LiFePO_4$ nanocrystals synthesized: (a) in the absence of organic molecules, (b) in the presence organic molecules. Inset images of (b) are SAED patterns of the $LiFePO_4$ nanocrystals bulk region and particle boundary respectively, (c) distinct lattice planes of selected particle in (b), and (d) EDS analysis of the particles.

supercritical water hydrothermal conditions, at 400 °C, the action of water leads to the partial conversion of SP^3 to SP^2 in diamond like carbon that is rich in SP^3 bonds and the almost complete transformation to SP^2 bonded amorphous carbon occurs above 600 °C [25].

3.3. Size and morphology of $LiFePO_4$

The morphology and the particle size of $LiFePO_4$ nanocrystals were studied in detail using FESEM and HR-TEM images. The FESEM image of the nanocrystals synthesized in the absence of organic molecules displayed spherical shaped particles ranging from 150 to 200 nm (Fig. 5a). The particles size was decreased with the addition of oleic acid molecules into the reaction system as shown in Fig. 5b. The histograms of the particle size distribution of the $LiFePO_4$ particles synthesized in the presence and absence of organic molecules were analyzed from the HR-TEM images and their plots are shown in Fig. 5c and d. This data further suggests that in the presence of organic molecules $LiFePO_4$ nanocrystals formed has a narrow particle size distribution with mean size of about 15 nm. In contrast, the $LiFePO_4$ nanocrystals formed in the absence of organic molecules show no control over the particle size displaying very wide range of size distribution with an average particle size of about 150 nm.

The HR-TEM images of $LiFePO_4$ nanocrystals synthesized in the absence and presence of organic molecules under SCW conditions are shown in Fig. 6. The $LiFePO_4$ particles synthesized in the absence of organic molecules are bigger in size and show a sharp surface edge without any carbon or organic layer (Fig. 6a). Whereas, the $LiFePO_4$ nanocrystals synthesized in the presence of the organic molecules are smaller than 15 nm (Fig. 6b). The distinct lattice planes in Fig. 6c and the SAED pattern in Fig. 6b (top inset) with bright spots of well defined diffraction pattern of olivine phase suggests that the good crystalline $LiFePO_4$ nanocrystals were formed under organic molecules assisted SCW conditions. An amorphous carbon layer with thickness of about 3–4 nm was observed on the particles surface (Fig. 6c). This was due to the generation of carbon on the particle surface by the decomposition of organic molecules under harsh supercritical water conditions during the synthesis. The nanoparticles surface having carbon layer is marked with blue dashed circle in Fig. 6b. The SAED pattern (bottom inset) in the same image indicates that it is an amorphous phase of carbon. The EDS analysis of the selected area in Fig. 6b is displayed in Fig. 6d, which confirms the presence of Fe and P elements. Fig. 6b also shows a small carbon peak which supports the above results that the thin coating present on the surface of $LiFePO_4$ is amorphous carbon. We further confirmed the uniform distribution of carbon on the surface by STEM mapping of carbon, oxygen, phosphorous and iron in the $LiFePO_4$– coated with 20% oleic acid, Fig. 7. The carbon distribution and carbon morphology affects its electrochemical performance [26].

In addition, we have also confirmed the residual amount of carbon in the $LiFePO_4$– sample coated with 20% oleic acid after heat treatment at 500 °C by TG-DTA analysis. The residual carbon amount found was about 10.5 wt. % (data not shown).

3.4. Formation of $LiFePO_4$

Supercritical water conditions provide a facile route to prepare the organic and/or carbon coated $LiFePO_4$. The $LiFePO_4$ nanocrystal formation under the organic molecules assisted supercritical water occurs in four steps as shown in Fig. 8. At first, sub-10 nm single crystal formation in a supercritical water [19]; secondly, the organic molecules miscible with high-temperature water forms homogenous phase, which is due to the lower dielectric constant of the water at its supercritical condition [27]; followed by the controlled nanocrystal growth that occurs by selective reaction of organic molecules with the specific inorganic crystal surface [28]; and finally by extending reaction time organic molecules covered on the surface was decomposed to form thin carbon coating on the $LiFePO_4$ surface [29]. Using organic ligand molecules that are mis-

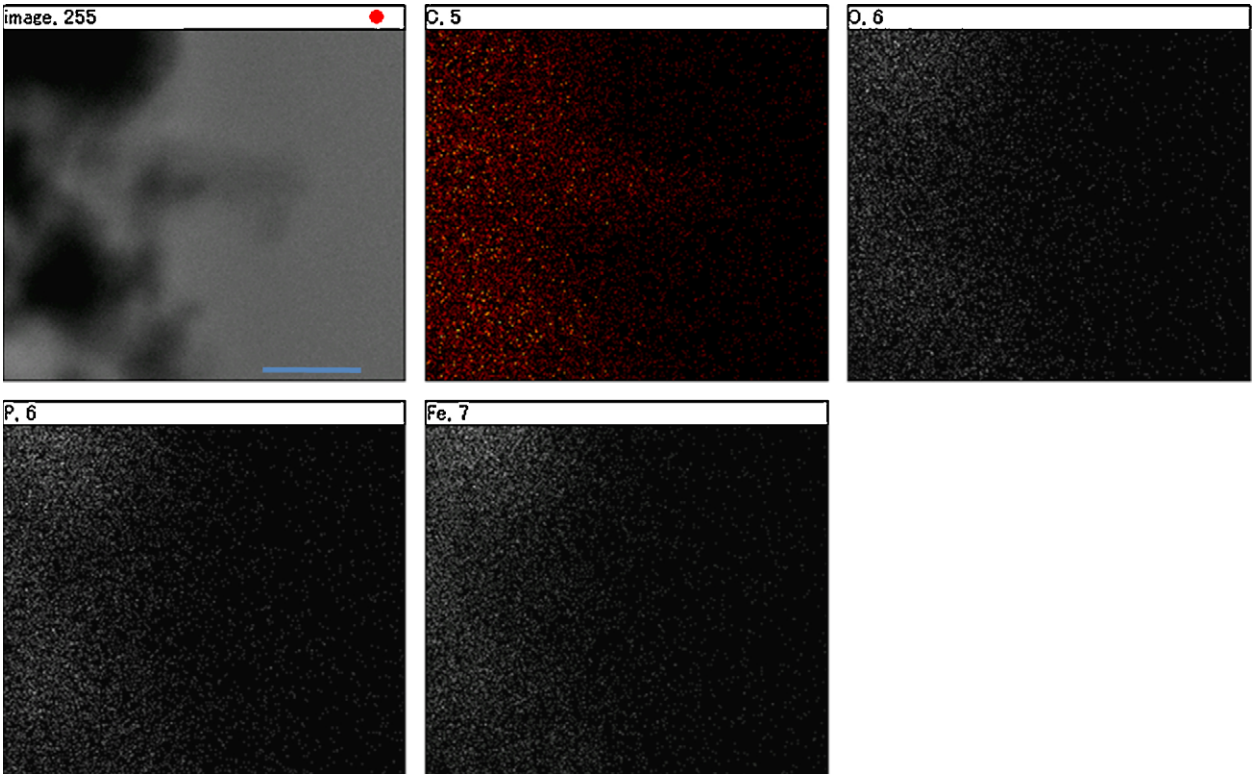

Fig. 7. STEM image and corresponding STEM maps of carbon, oxygen, phosphorous and iron in $LiFePO_4$ coated with 20% oleic acid.

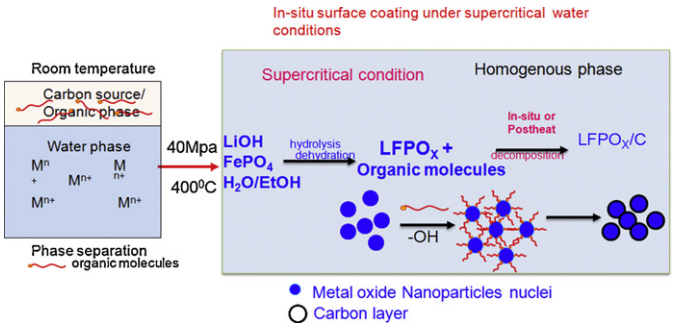

Fig. 8. Reaction model showing homogeneous phase formation, $LiFePO_4$ formation, organic modification and $LiFePO_4$/C formation under SCW.

cible with SCW, the organic modified $LiFePO_4$ nanocrystals with 15–20 nm size and well-dispersed particles were obtained as shown in Fig. 6.

3.5. Electrochemical property of $LiFePO_4$

Electrochemical performance measured for $LiFePO_4$/C sample is shown in Fig. 9. As prepared sample in Fig. 9a shows capacity up to 65 mA g^{-1}. The low capacity of this sample indicates that the surface of the as prepared sample was covered with amorphous carbon, in addition, some of the organic ligand molecules remained on the surface affecting the conductivity of sample to result in a poor capacity. The heat treated sample at 500 °C under Ar and H_2 gas exhibited the typical charge–discharge curves of the Li–$LiFePO_4$/C cells cycled between 2 and 4.0 V at a current of 0.1 C (Fig. 9b). This indicated the single charge–discharge plateau around 3.5 V versus Li/Li^+ suggesting a simple lithium intercalation–deintercalation reaction in pure olivine $LiFePO_4$ phase, as reported previously by Padhi et al. Generally, the presence of impurity phases such as $Li_3Fe_2(PO_4)_3$ and others show a lower voltage plateau at 2.0–2.6 V, however, in the present study, the absence of such plateau suggests that there was no active impurity phase in the $LiFePO_4$/C. This sample exhibited highest discharge capacity of 155 mAh g^{-1}, about 92% of the theoretical capacity of $LiFePO_4$.

In order to improve the rate capability of the $LiFePO_4$ samples we added a small amount of (5 wt. %) of conductive carbon nanotubes (CNT) in the starting precursor. The $LiFePO_4$ and CNT composites were synthesized under the same SCW conditions and heat treated at 500 °C under Ar and H_2 gas. The

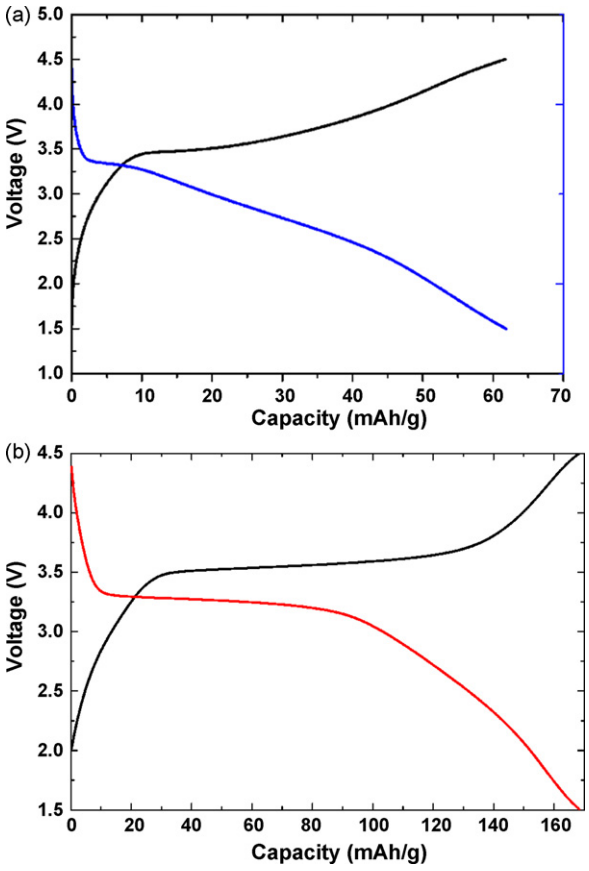

Fig. 9. Charge/discharge profiles of $LiFePO_4$/C composite at 0.1 C rate: (a) as-prepared sample, (b) heat treated at 500 °C for 2 h under Ar and H_2 gas atmosphere.

resultant $LiFePO_4$/CNT sample morphology is shown in Fig. 10. The as-prepared sample in Fig. 10a indicates that the $LiFePO_4$ nanocrystals have deposited on the surface of CNT. The heat treated $LiFePO_4$/CNT sample shows that the surface of $LiFePO_4$ was completely covered with CNT and carbon, which improved the connection between the nanocrystals of $LiFePO_4$/C. This sample showed the improved electrochemical performance. Fig. 11 presents the charge–discharge profiles of $LiFePO_4$/CNT nanocomposite at various discharge rates ranging from 1 to 8 C. The capacities of $LiFePO_4$/CNT decreased from 165 to 100 mAh g^{-1} by increasing

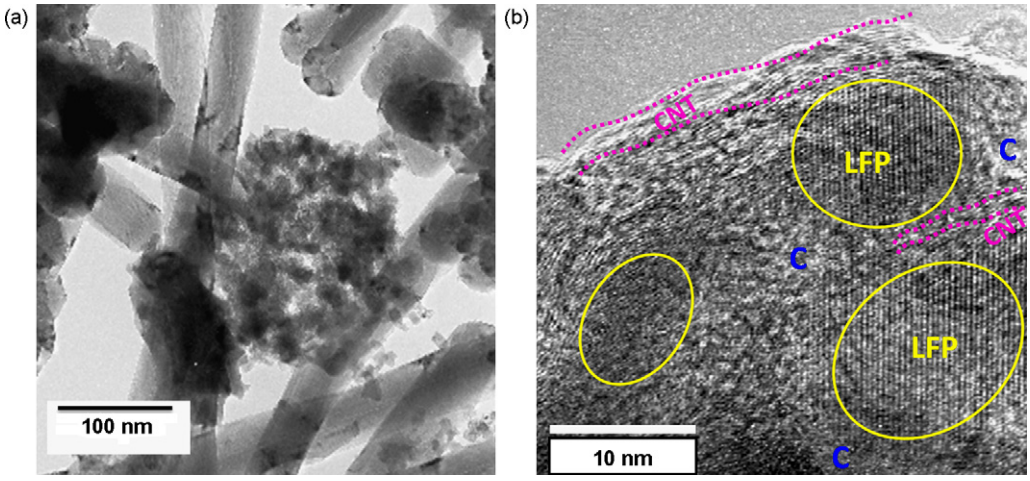

Fig. 10. $LiFePO_4$/CNT sample: (a) as prepared with carbon nanotubes (CNT) under SCW 400 °C and (b) heat treated at 500 °C under Ar and H_2 atmosphere for 2 h.

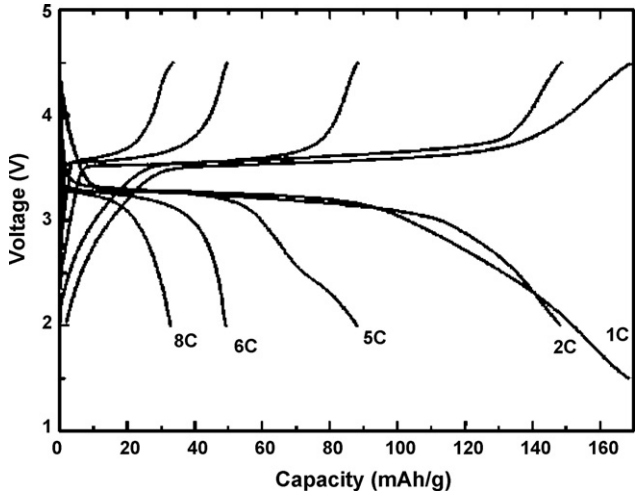

Fig. 11. The discharge profiles of $LiFePO_4$/CNT nanocomposite at various discharge rates ranging from 1 to 8 C. The sample was synthesized at 400 °C in 10 min by SCW method followed by heat treatment at 500 °C.

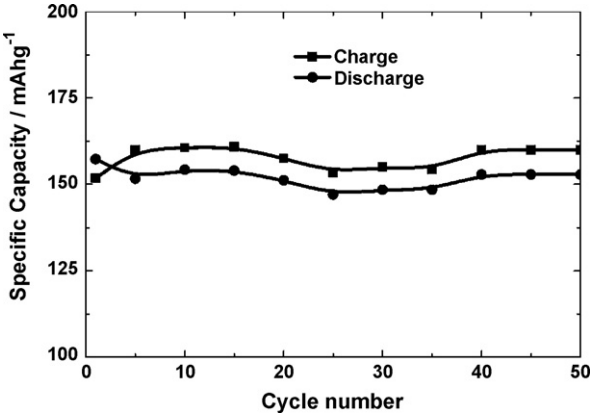

Fig. 12. Cycling performances of the $LiFePO_4$/CNT nanocrystals synthesized with addition of CNT at 400 °C in 10 min by SCW method followed by heat treatment at 500 °C. The measurement was at 0.5 C charge and discharge rates.

the discharge rates from 1 to 5 C. About 89% of theoretical capacity was retained at 1 C. Although the specific capacity decreases with increase in current rate, the capacity retention remains very good up to 2 C. This decrease in capacity with higher rate can be attributed to the presence of partial amorphous carbon and thick carbon coating on the $LiFePO_4$ surface. However, this sample displayed relatively good cyclic performance with an apparent specific discharge capacity 155 mAh g^{-1} even after 50 cycles at 0.5 C charge/discharge rate (Fig. 12). This rate performance and cycling stability of the $LiFePO_4$/CNT nanocomposite could be attributed to the fact that nanosize particle with high crystallinity and improved conductivity through an optimized conductive carbon surface.

In spite of the good electrochemical performance of the presently synthesized material, advantages of the organic molecules assisted SCW system for the size controlled synthesis of $LiFePO_4$ nanocrystals have been demonstrated through this study.

4. Conclusion

We have reported a novel route for synthesis of $LiFePO_4$/C nanocrystals (<15 nm) by organic molecules assisted SCW synthesis. The XRD, Raman, HR-TEM and EDS measurements revealed that the $LiFePO_4$/C nanocrystals composite was formed under organic molecules assisted SCW conditions. The used organic molecules were coated onto the surface of the $LiFePO_4$ nanocrystals and inhibited the growth of particles resulting in drastic change in the particle size from 150 to 200 nm to 15–20 nm. The surface coated organic molecules were transformed to carbon layer during heat treatment at relatively lower temperature (500 °C) under Ar and H_2 gas for 2 h, resulting in the $LiFePO_4$/C nanocomposite. About 97% theoretical capacity of $LiFePO_4$ was achieved with very good cyclic performance. Addition of CNT during the synthesis of $LiFePO_4$ under SCW condition had significant effect in improving the conductive coating surface. A further study on the $LiFePO_4$/CNT is under progress and will be reported shortly.

Acknowledgement

This research is supported by NEDO Grants under the program "Development of High Power and High Energy Li-ion Secondary Battery by Nanofabrication Li–host composites".

References

[1] K. Shiraishi, K. Dokko, K. Kanamura, J. Power Sources 146 (2005) 555.
[2] A.K. Padhi, K.S. Nanjundaswamy, J.B. Goodenough, J. Electrochem. Soc. 144 (1997) 1188.
[3] H. Huang, S.-C. Yin, L.F. Nazar, Electrochem. Solid State Lett. 4 (2001), 10, A170.
[4] A. Yamada, S.C. Chung, K. Hinokuma, J. Electrochm. Soc. 148 (2001) A224.
[5] N. Ravet, Y. Chouinard, J.F. Magnan, S. Besner, M. Gauthier, M. Armand, J. Power Sources 97–98 (2001) 503.
[6] Y. Wang, J. Wang, J. Yang, Y. Nuli, Adv. Funct. Mater. 16 (2006) 2135.
[7] S. Franger, F.L. Cras, C. Bourbon, H. Rouault, Electrochem. Solid-State Lett. 5 (2002) A231.
[8] C.W. Kim, M.H. Lee, W.T. Jeong, K.S. Lee, J. Power Sources 146 (2005) 534.
[9] J. Yang, J.J. Xu, Electrochem. Solid-State Lett. 7 (2004) A515.
[10] G.X. Wang, S. Bewlay, S.A. Needham, H.K. Liu, R.S. Liu, V.A. Drozd, J.-F. Lee, J.M. Chen, J. Electrochem. Soc. 153 (2006) A25.
[11] K.S. Park, K.T. Kang, S.B. Lee, G.Y. Kim, Y.J. Park, H.G. Kim, Mater. Res. Bull. 39 (2004) (1803).
[12] K.S. Park, J.T. Sun, H.T. Chung, S.J. Kim, C.H. Lee, H.G. Kim, Electrochem. Commun. 5 (2003) 839.
[13] S. Yang, P.Y. Zavalij, M.S. Whittingham, Electrochem. Commun. 3 (2001) 505.
[14] S.-T. Myung, S. Komaba, N. Hirosaki, H. Yashiro, N. Kumagai, Electrochim. Acta 49 (2004) 4213.
[15] T.-H. Cho, H.-T. Chung, J. Power Sources 133 (2004) 272.
[16] J. Barker, M.Y. Saidi, J.L. Swoyer, J. Electrochem. Soc. 6 (2003) A53.
[17] I. Belharouak, C. Johnson, K. Amine, Electrochem. Commun. 7 (2005) 983.
[18] K. Konstantinov, S. Bewlay, G.X. Wang, M. Lindsay, J.Z. Wang, Electrochim. Acta 50 (2004) 421.
[19] T. Adschiri, Y. Hakuta, K. Arai, Ind. Eng. Chem. Res. 39 (2000) 4901.
[20] D. Rangappa, S. Ohara, T. Naka, A. Kondo, M. Ishii, T. Adschiri, J. Mater. Chem. 129 (2007) 11066, 36.
[21] T. Adschiri, K. Kanazawa, K. Arai, J. Am. Ceram. Soc. 75 (1992) 2615.
[22] K. Dokko, K. Shiraishi, K. Kanamura, J. Electrochem. Soc. 152 (2005), 11, A2199.
[23] M.B. Christopher, F. Roger, Spectrochem. Acta Part A 65 (2006) 44.
[24] M.M. Doeff, Y. Hu, F. McLarnon, R. Kostecki, Electrochem. Solid-State Lett. 6 (2003) A207.
[25] J.M. Calderon-Moreno, Diamond Relat. Mater. 15 (2006) 958.
[26] R. Dominko, M. Gaberscek, J. Drofenik, M. Bele, S. Pejovnik, J. Jamnik, J. Power Sources 119–121 (2003) 770.
[27] D. Rangappa, T. Naka, A. Kondo, M. Ishii, T. Adschiri, J. Am. Chem. Soc. 129 (2007) 11064, 36.
[28] (a) P.E. Savage, Chem. Rev. 99 (1999) 603;
(b) N. Akiya, P.E. Savage, Chem. Rev. 102 (2002) 2725.
[29] J. Zhang, S. Ohara, M. Umetsu, T. Naka, Y. Hatakeyama, T. Adschiri, Adv. Mater. 19 (2007) 203.